Chapter 2

Detection of defects in fabric using sub-image based singular value decomposition

2.1. Introduction

This chapter proposes a method of fabric defect detection by using the sub image-based singular value decomposition (SVD), which has not been evaluated fully for defect detection in fabrics. SVD is based on ortho-normal decomposition of a matrix. By considering an image as a matrix, SVD is used to decompose the image and then obtain a diagonal matrix and two orthogonal matrices of the singular vectors. The ordered entries of the diagonal matrix are singular values. The global information (or the approximation) of the image can be represented by a few singular values of large magnitude. This method thus can be applied for the removal of global information of the fabric image i.e. the interlaced grating structure and can preserve the local information i.e., the information of fabric defects.

Singular value decomposition (SVD) [119] has been successfully applied to many image processing problems [120]. Usual applications include image enhancement and restoration [121, 122], hiding, coding, and water marking [123, 124]. Few studies have been proposed using SVD for texture analysis [125]. Higher order SVD for dynamic texture analysis has been proposed recently [126]. Since SVD method identifies the dimensions along which the data point shows the maximum variation; the singular values obtained by using SVD method give the information about the distribution of data in a fabric image. Therefore, the elimination of prominent singular values helps in the detection of defects in fabrics while reconstructing the image with lesser number of singular values. SVD technique also weakens the impact of illumination variations and deviations in weft-warp grating structures. [127, 128, 129] have shown that distributions of data are changed due to the fabric defects. However, the use of SVD was severely limited because of a large number of computations required for calculating singular values and singular vectors of large image matrices.

Normally fabric defect, being small in comparison to the entire fabric area, the sub image-based SVD method gives better capability in the detection process, while time complexity of operating with matrix of large size is eliminated [130]. If the image is broken up into smaller sub images and each is processed separately, the overall processing time is much reduced. The sub image-based SVD procedure of defect detection in liquid crystal display (LCD) panel has been reported by Lu and Tsai [131]. However, while applying the technique for the defect detection in fabrics some distinctions can be made. The grating structure of the LCD panel is absolutely regular in contrast to the weft-warp interlaced grating structure of the fabric which is not so regular. Hence, the straight forward application of the method proposed for defect detection in LCD panel as reported in [131] may not be advantageous while applying for the defect detection in fabrics.

In this work, the sub image-based SVD method is generalized in such a way so that the size of sub image is selected adaptively by identifying a region of interest (ROI) so that the time complexity for a large image size is reduced. The proposed technique identifies different types of fabric defects on different types of fabric images after suitable post processing for binarization followed by edge detection to yield edge map of the defect.

2.2. Mathematical background of sub image based SVD method

Let the p th gray scale fabric image of a fabric class of size $(M \times N)$, be denoted as $f_p \in \Re^{(M \times N)}$, such that $1 \le p \le P$, where P is the total number of fabric image. Considering, $M > N$, f_p can be decomposed into three matrices U_p, S_p, V_p in the following way,

$$f_p = U_p . S_p . V_p^T \tag{2.1}$$

where, $U_p = [u_{1p}, u_{2p}, ..., u_{Mp}]$ is an $(M \times M)$ orthogonal matrix consisting of M singular vectors, which are the columns of U_p and T denotes the transpose operation.

$V_p = [v_{1p}, v_{2p}, ..., v_{Np}]$ is another $(N \times N)$ orthogonal matrix consisting of N singular vectors (columns of V_p). $S_p \in \Re^{(M \times N)}$ is a real pseudo-diagonal $(M \times N)$ matrix, whose diagonal consists of positive singular values σ_{ip} and all other elements are zeros. All singular values are arranged in descending orders such that $\sigma_{1p} > \sigma_{2p} > ......\sigma_{Np} > 0$.

It may be noted that the square of singular values are the eigen values of the covariance matrix $f_p . f_p^T$. The use of matrix SVD characteristics of the extract is stable, shift invariant, transpose invariant and rotation invariant. Without encountering much error f_p can be approximated in terms of rank r of the matrix as,

$$f_p \approx U_r . S_r . V_r{}^T \tag{2.2}$$

The rank r-approximation of f_p is interesting in the sense of packing the maximum energy. f_p has $(M \times N)$ entries and the approximate rank image has $(M + N + 1)r$ entries and S_r is the $(r \times r)$ top left sub matrix representing singular values. U_r consists of the first r columns of U_p and V_r^T, the first r rows of V_p^T. It can be seen that the error of the approximation decreases toward zero in the 2-norm sense. Therefore, it often turns out for defect detection in fabrics that even with small r, the rank approximation gets most of the energy of fabric image f_p and is adequate for defect detection. Instead of $(M \times N)$ entries, the image has now $[2(M+N)r+r]$ entries. In the following discussion only rank approximated images are used for further analysis.

A fabric image consists of bidirectional (usually orthogonal) interlaced and repetitive structural pattern of weft and warp yarns. Therefore, this grating pattern dominates in the whole image of fabric. In general, singular values of larger magnitude associated with small singular numbers represent the global approximation of the fabric image. This fact is reflected in SVD, where the magnitude of only a few larger singular values will dominate and all others singular values have magnitudes close to zero.

Figure 2.1 shows a set of synthetically generated fabric images and actual woven fabric images with their corresponding plots of magnitudes of 10 largest singular values. It can be seen from Figure 2.1 that the magnitude of first singular value dominates all other values associated with higher singular numbers and the magnitudes take a sharp change at the singular number 2. From the plots it is also evident that it is difficult to distinguish between the weave patterns of fabric except when the pattern is panama type weave.

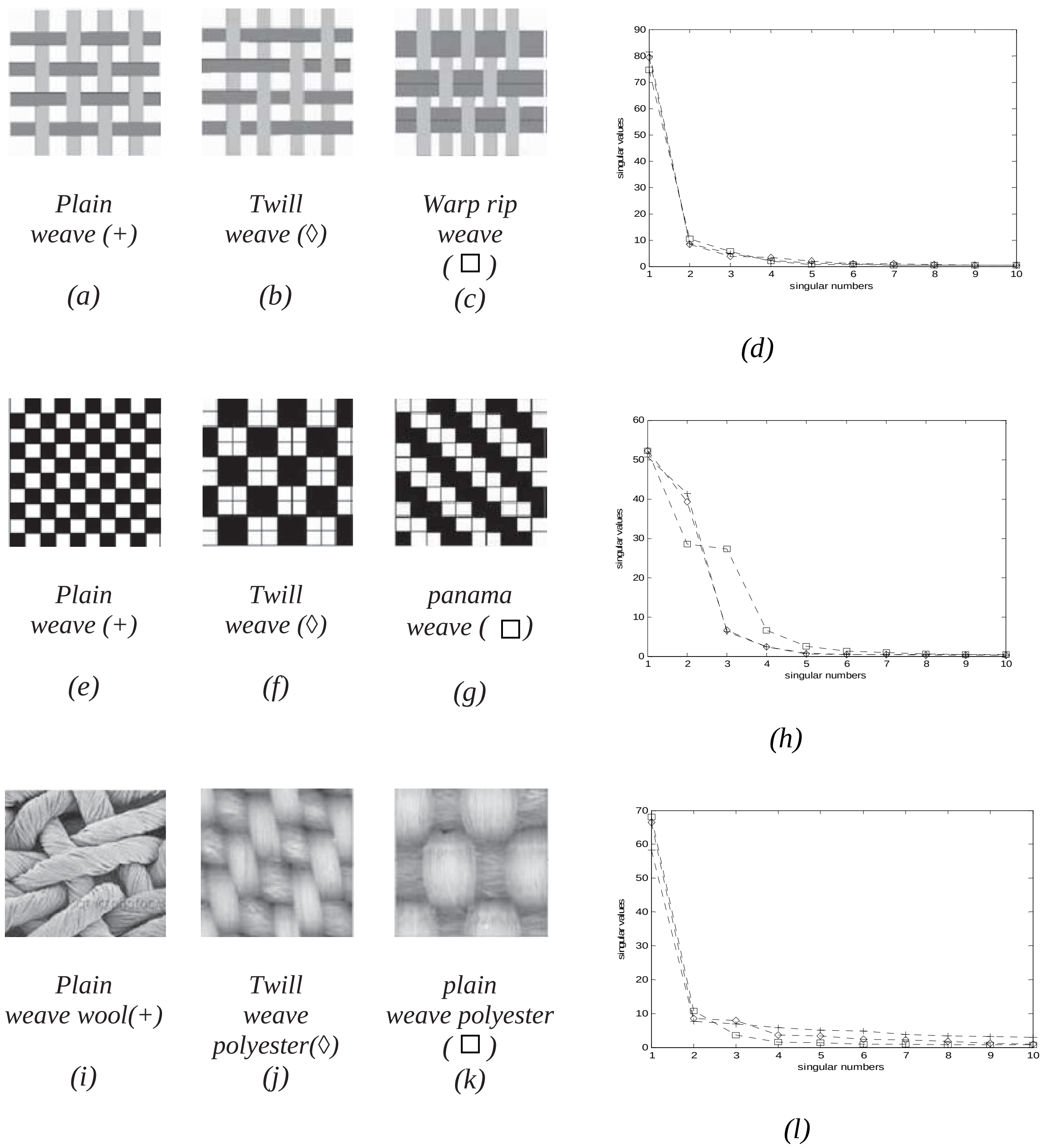

Figure-2.1: Synthetically generated fabric images (first and second rows) and actual fabric images (third row) and their SVD plots up to 10 singular numbers (fourth column).

Further, when the fabric structure changes drastically (images of third row of Figure 2.1) the magnitude of higher singular values shows appreciable change. It may be concluded that the distribution of singular value follows a general pattern due to weft-warp interlaced grating structure though no distinctive evidence of physical nature of structure of irregularities can be predicted.

The reverse process of retrieving the fabric image from the knowledge of U_r, S_r, V_r^T is possible. It has been found that during reconstruction process the rank-approximated image performs equally well. A new fabric image can be reconstructed by manipulation of singular values according to the desired properties. For example, the fabric image $f_p|_{rec}$, reconstructed by excluding k singular numbers sorted in increasing order as $\sigma_{(i+1)p} < \sigma_{ip}$ is given by,

$$f_p|_{rec} = U_p . S_p|_{rec} . V_p^T \tag{2.3}$$

where $U_p = [u_{1p}, u_{2p}, ..., u_{Mp}] \in \Re^{(M \times M)}$ is an orthogonal matrix consisting of M singular vectors u_{ip} and $V_p = [v_{1p}, v_{2p}, ..., v_{Np}] \in \Re^{(N \times N)}$ is an orthogonal matrix consisting of N singular vectors v_{ip} . $S_p|_{rec}$ is the pseudo-real diagonal matrix of the dominant singular values where singular numbers k >10 are excluded.

The effect of illumination on the reconstructed image is weak and the change in the reconstructed image due to illumination variations is proportionally reduced. This property of proportional change helps in the recognition process. Moreover, most of the energy associated with singular values can be preserved by using few most significant basis elements. It is readily seen that the reconstructed images approach to the original image with increasing the number of basis elements. If the number is bigger (usually >5), the difference between the reconstructed fabric image and the original fabric image is small. However, when dealing with fabric images of many classes, one needs to normalize the magnitudes of singular values before any processing. Denoting $\underline{\sigma_{ip}}$ as the normalized magnitude of i th singular value of p th sample of a class of fabric, where $i = 1,........, r$, $\underline{\sigma_{ip}}$ is given by,

$$\underline{\sigma_{ip}} = \frac{\sigma_{ip} - \mu_{\sigma p}}{\delta_{\sigma p}} \tag{2.4}$$

where $\delta_{\sigma p}$ is the standard deviation of magnitude of all singular values and $\mu_{\sigma p}$ is the mean magnitude of singular values which is given by,

$$\mu_{\sigma p} = \frac{1}{r} \sum_{i=1}^{r} \sigma_{ip} \tag{2.5}$$

2.3 Finding the region of interest (ROI) by adaptive partitioning

Since a defect may occur only in a small portion of the entire fabric, the region of interest (ROI) in fabric image is identified to reduce the computational cost. Evidently, ROI should contain the defective part of the fabric. A generalized split scale rule of partitioning is proposed to identify ROI.

If f_p is the entire fabric image, ROI part of the fabric image is designated as $f_p\,|_{\alpha,\beta}$ where $\alpha = 1,2,.........,d$, is termed as the split-scale partition number and maximum value of $\beta = 2^{2(\alpha-1)}$. Evidently, $f_p\,|_{1,1}$ is the split scale 1 fabric image which is the un-partitioned image f_p. Split scale 2 partitioned image, consists of four sub images $f_p\,|_{2,1}$, $f_p\,|_{2,2}$, $f_p\,|_{2,3}$, $f_p\,|_{2,4}$. Similarly, the split scale 3 partitioned image shall consist of 16 sub images, when each sub image of split scale 2 is further divided into split scale 2. Similarly, split scale 4, 5, and higher split scales can be designed following the same procedure. If M and N are even numbers, then the size of the sub image can be expressed in terms of the split scale as $[\frac{M}{2^{(\alpha-1)}} \times \frac{N}{2^{(\alpha-1)}}]$. For an image of any size, odd or even M or N , the division by $2^{(\alpha-1)}$ can continue till the residue is an odd number. For an image of square size $M = N$, the minimum size of partitioned sub image can be (2×2), while for rectangular image $(M > N)$, the minimum image size can be (1×3), when M is an even and N is an odd number.

The entire fabric image f_p can be expressed in terms of the split scale partitioned sub images as,

$$f_p = [f_p|_{\alpha,\beta}] \tag{2.6}$$

In the fabric image, the intensity value of the pixels at the defective part varies appreciably from those at the defect free repetitive part of the fabric. This gives a major advantage of using an adaptive partitioning technique to find ROI which contains the defect. Initially, the fabric image is partitioned into split scale 2 thus producing four sub images. Then each of the sub images is correlated with a defect-free template image f_t of same size and same fabric class.

Evidently, all sub images will be highly correlated with the template, if none of the sub images contains a defect. The partitioned sub image, whose correlation with the template is low is split again into split scale 2 and correlated with a defect-free template of same size. The highly correlated (see in the next paragraph) partitioned sub images are not split and all pixel's gray values are put to 1 (white). In this way, ROI is obtained, which contains only the defective part and the region outside ROI is white. Figure 2.2 shows two such examples of generating ROI.

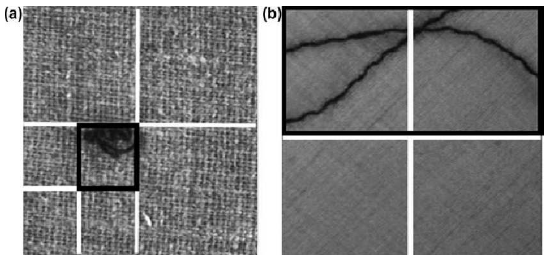

Figure- 2.2: Split scale image partitioning technique (a) multiple iterations of splitting at split scale 2 and (b) single iteration of splitting at split scale 2.

There are many techniques of obtaining correlation value of two images of which sum of squared difference (SSD) technique is simplest and computationally efficient. The intensity values of the sub image after split $f_p|_{\alpha,\beta}$ and a template image of defect-free fabric f_t of the same size and of same fabric class are arranged in two one-dimensional data lists. Then the sums of squared difference of Euclidean distance between the corresponding pixels in the two images are calculated. SSD is given by,

$$SSD = \sum_{y_0=1}^{n_0} \sum_{x_0=1}^{m_0} [f_p|_{\alpha,\beta}(x_0, y_0) - f_t(x_0, y_0)]^2 \quad (2.7)$$

where, $f_p|_{\alpha,\beta}(x_0, y_0)$ is the pixel value of split sub image at a coordinate (x_0, y_0) at split scale α, $f_t(x_0, y_0)$ is the pixel value of template of equal size with the split sub image at a coordinate (x_0, y_0).

Note that the value of SSD close to zero (or below a threshold value) indicates the best match if the test sub image is defect free. SSD value above the threshold value indicates the presence of defect in the test sub image and the sub image in question is split again. The number of partitioned sub images is set automatically. However, the template sub image of defect-free fabric has to be resized after each partition. The adaptive technique of finding ROI partitioning as proposed is efficient and takes little time for computation.

In practice, it is not possible to reduce the size of sub image in ROI indefinitely, as the size depends on the intensity value of the image, the coarseness of the fabric, the type of weave, and the type of defect. Thus the partitioning is stopped after a certain iterations, when the SSD becomes enough high.

2.4. Removal of interlaced grating structure of fabric in ROI

It may be appreciated that though ROI of the fabric is comparatively small than the original fabric image, yet depending on the orientation and size of the defect, it may still contain the defect superimposed on grating structure of the image. Therefore, it is necessary to filter out the grating structure by removing the singular values responsible for the grating structure. Moreover, the extraction of defect by straightforward SVD is still computationally intensive. It is observed that the numbers of singular values representing the fabric background decreases dramatically with the decrement in the size of the fabric sub images, though there is no linear relationship between them. In other words, as the size of the fabric sub image decreases the background information carried by the first few dominant singular numbers increases.

The exact number of singular values which can be eliminated is obtained from the knowledge of the defect-free template image f_t of the size of ROI. Let the size of ROI is denoted by $(m_0 \times n_0)$. To reduce the computational complexity, the defect-free template image is divided into a number of small non overlapped sub images of size $(m \times n)$, such that $D = (\frac{m_0}{m} \times \frac{n_0}{n})$ numbers of non-overlapped sub images are created. The i th average normalized singular value of all sub images of the fabric template of size of ROI belonging to a fabric class is calculated as,

$$\overline{\sigma}_i = \frac{1}{D} \sum_{y=1}^{\frac{n_0}{n}} \sum_{x=1}^{\frac{m_0}{m}} \underline{\sigma}_i(x, y) \tag{2.8}$$

where, $\underline{\sigma}_i(x, y)$ is the ith normalized singular value obtained from the (x, y) th non overlapped fabric sub image taken from the fabric template of a fabric class. $\underline{\sigma}_i(x, y)$ is given by,

$$\underline{\sigma}_i(x,y) = \frac{\sigma_i(x,y) - \mu_\sigma(x,y)}{\delta_\sigma(x,y)} \tag{2.9}$$

where $\mu_\sigma(x,y)$ is the mean, $\delta_\sigma(x,y)$ is the standard deviation of all the singular values obtained from (x,y)th non-overlapped fabric sub image and $\sigma_i(x,y)$ is the ith singular value obtained from the (x,y) th non-overlapped fabric sub image taken from the fabric template of a fabric class.

The numbers of positive average normalized singular values carry the information of fabric background. It has also been observed that the most dominant singular numbers required to be eliminated for the removal of the fabric background in the reconstructed fabric image is dependent on the size of the fabric sub image.

Figures 2.3(a) and (b) show the plot of average normalized singular values for a fabric image of size (128×128) of a particular fabric class for different sizes of sub images.

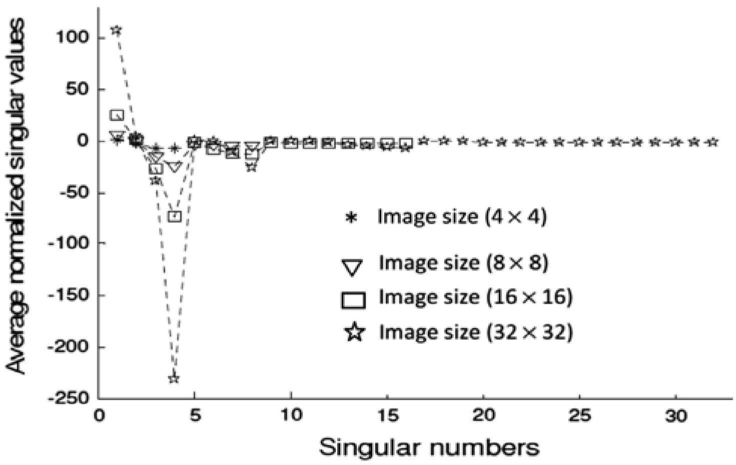

Figure-2.3(a): Plot of average normalized singular values for sub image size of (4×4), (8×8), (16×16), (32×32).

The corresponding dominant singular numbers, having positive average normalized singular values and to be removed for the removal of interlaced structure of the fabric become 2, 3, 9, and 16 respectively. For sub image size of (64×64) and (128×128) dominant singular numbers become 42 and 98 respectively and hence are not of any use. As it is not possible to reduce the size of sub image in ROI indefinitely so, it is necessary to find the optimum singular numbers to be eliminated to remove the interlaced grating structure from ROI by selecting a sub image of proper size.

.

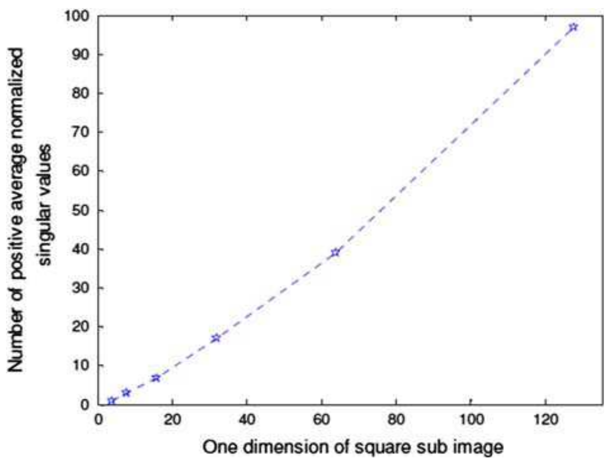

Figure-2.3(b): Plot of number of positive average normalized singular values against dimensions of square image.

Let for a fabric class, the numbers of positive average normalized singular values is k_p for the sub image size of $(m\times n)$, which carries the information of the interlaced grating structure of the fabric under *ROI* region of size $(m_0\times n_0)$. To remove the grating structure SVD method is applied on each sub image of size $(m\times n)$ and the corresponding singular values are determined. Let i th most dominant singular value of the defect-free sub image of a fabric class having size $(m\times n)$ be σ_i^t, where i varies from 1 to k_p and $\sigma_{ip}^{ROI}(x,y)$ is the i th singular value of the (x,y) th fabric sub image of ROI part of p th fabric image of a fabric class, which contains a defect and the grating structure is not suppressed. Also let $\sigma_{ip}^{m}(x,y)$ is the ith singular value of the (x,y)th reconstructed fabric sub image of pth fabric image of a fabric class, in which up to k_p singular numbers are removed for suppression of the interlaced grating structure, then,

$$\sigma_{ip}^{m}(x,y) = abs[\sigma_{ip}^{ROI}(x,y) - \sigma_{i}^{t}] \qquad (2.10)$$

where i varies from 1 to k_p, x and y vary from 1 to $\frac{m_0}{m}$ and 1 to $\frac{n_0}{n}$, respectively.

From the modified singular values of the (x,y) th sub image of the background suppressed pth fabric image belonging to a fabric class, the diagonal matrix $S_{p}^{m}(x,y)$ is formed by padding with suitable numbers of zero as,

$$S_{p}^{m}(x,y) = diag\,[\sigma_{1p}^{m}(x,y), \sigma_{2p}^{m}(x,y), ..., \sigma_{k_p p}^{m}(x,y), \sigma_{(k_p+1)p}^{ROI}(x,y), ..., \sigma_{mp}^{ROI}(x,y)] \qquad (2.11)$$

The background removed (x,y)th reconstructed fabric sub image is obtained as,

$$f_{pROI}|_{rec}(x,y) = U_{pROI}(x,y).S_{p}^{m}(x,y).V_{pROI}(x,y)^{T} \qquad (2.12)$$

where $U_{pROI}(x,y)$ and $V_{pROI}(x,y)$ are the left and right singular matrices of the (x,y)th sub image of ROI part of the pth fabric image of the fabric class.

Finally, the background-free reconstructed pth fabric image of the defect of the fabric class is obtained as,

$$f_{prec} = [f_{pROI}|_{rec}(x,y)] \qquad (2.13)$$

2.5. Post-processing for recovery of the image of defect

Post-processing of resulting image is necessary as the image may contain noise and some unconnected parts since the fabric sub images may not be totally identical. To obtain the image of the defect from the p th reconstructed gray fabric image of a fabric class, f_{prec} , binarization of the gray image is done. A threshold value θ is considered which operates on f_{prec} to yield a binary image of defect in the following way,

$$\begin{aligned} &if \quad f_{pROI}\ |_{rec}\ (x,y)\,|_{(x_0,y_0)} > \theta\ ; \quad f_{pb}(x,y)\,|_{(x_0,y_0)} = 1 \\ &else \qquad\quad f_{pb}(x,y)\,|_{(x_0,y_0)} = 0 \end{aligned} \tag{2.14}$$

where, $f_{ROI}\ |_{rec}\ (x,y)\,|_{(x_0,y_0)}$ is the intensity of (x,y) th reconstructed fabric sub image at a coordinate (x_0, y_0) and $f_{pb}(x,y)\,|_{(x_0,y_0)} \in \{0,1\}$ is the intensity of (x,y) th reconstructed fabric sub image at a coordinate (x_0, y_0) .

The binary defect image is given by,

$$F_{pb} = [\, f_{pb}(x,y)|_{(x_0,y_0)}\,] \tag{2.15}$$

The binary image of defect may still contain some unconnected parts which may result from the reconstruction process through the elimination of few singular values up to k_p . The resultant image after binarization is processed to indicate the edges of the defect by a standard gradient operator [132]. Thus, the edge map F_{ped} of the defect in the p th fabric of a fabric class is obtained.

2.6. Test result on TILDA database

The developed system is tested on the TILDA [118] database. The proposed method is tested on 460 fabric images with defects taken from three different fabric classes namely fine, medium, and coarse fabric class and the defects are detected for 433 samples. Apparently the detection rate, as given by the ratio of the number of defective samples correctly detected to the total number of defective samples is calculated as 94.13% and the apparent detection success rate defined as the ratio of total number of samples correctly detected to the total number of samples is 94% when 40 more defect-free samples are also tested by the system making total number of samples tested as 500. The false alarm rate, defined as the ratio of numbers of defect free samples detected as defective to the total numbers of defect free samples is 7.5%. The test results are shown in Table 2.1. Figure 2.4 shows some representative test results, where some defects are shown in test fabrics of fine, medium, and coarse classes.

The first column is the images of defective fabrics. The second column shows the ROI obtained by adaptive split scale partitioning. The third column shows the images of ROI after reconstruction by eliminating few dominant singular values. The last column shows the edge map of the defect after post-processing.

From the test result true positive (TP), false positive (FP), false negative (FN) and true negative (TN) values are estimated as 94.13%, 7.5%, 5.9% and 92.5% respectively. Thus the actual detection success rate given by the ratio of summation of TP and TN to the summation of TP, FP, FN and TN becomes 93.32%.

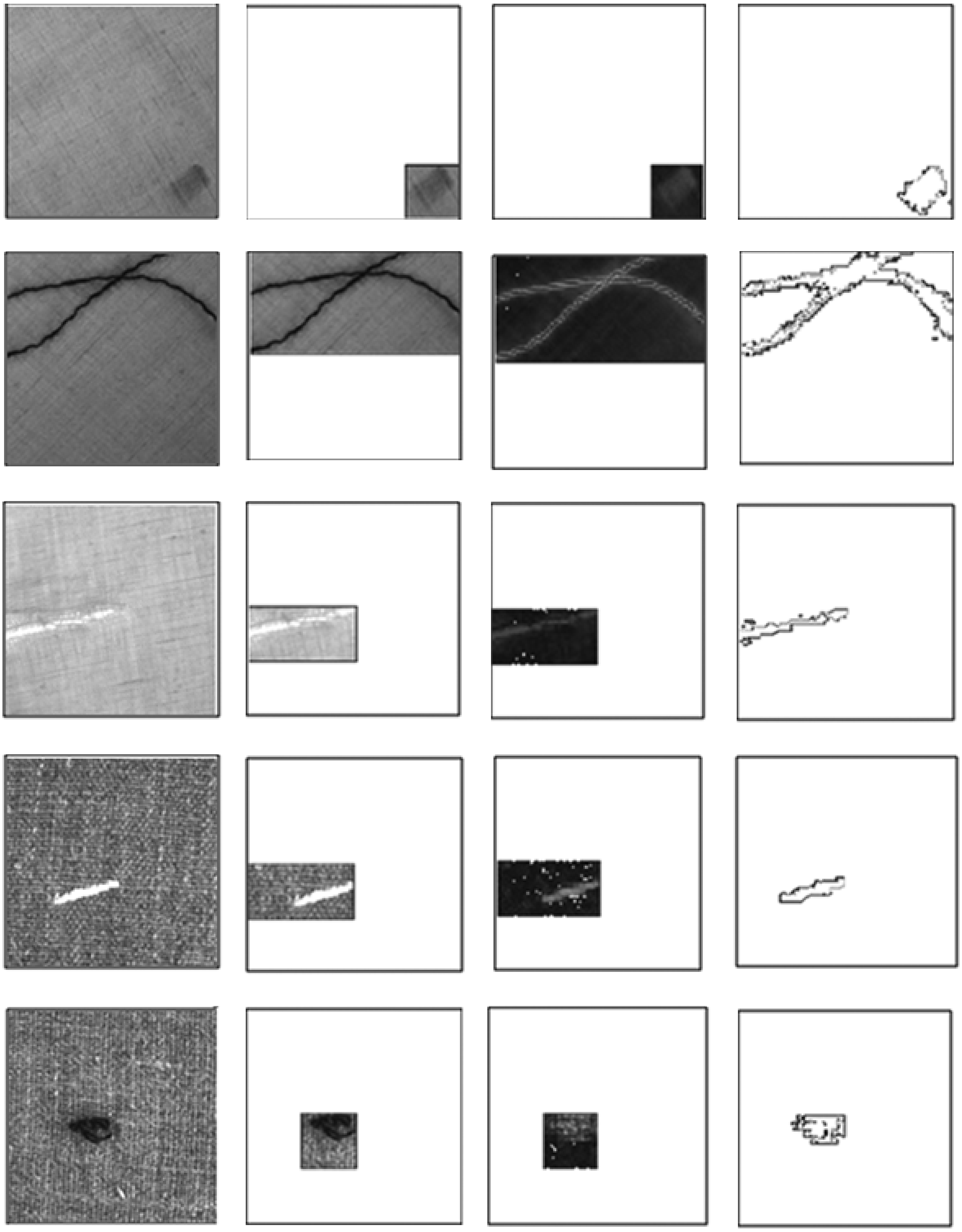

Figure-2.4: Images of test results; column 1: fabric image; column 2: partitioned image by split scale adaptive partitioning; column 3: images after SDV; column 4: images of defects after post-processing.

Table- 2.1: Test results on TILDA database.

Types of defects	Fine fabric		Medium fabric		Coarse fabric	
	No. of sample tested	No. of defect detected	No. of sample tested	No. of defect detected	No. of sample tested	No. of defect detected
Snarls/Loops	7	5	3	3	0	0
Small holes	17	17	19	19	9	9
Slub/ Fly	43	41	57	55	15	12
Thick yarn	46	42	0	0	10	8
Thin places	4	4	2	2	0	0
Knots	7	7	5	5	3	3
Broken pick	0	0	10	8	23	20
Short pick	7	6	10	8	20	18
Oil mark	35	35	26	26	33	33
Snag	7	7	10	10	18	18
Defect free	5	5	5	4	4	3
Total	**178**	**169**	**147**	**140**	**135**	**124**

2.7. Conclusion

The proposed method is based on image reconstruction scheme using SVD. In order to speed up the computation of SVD, a region of interest (ROI) encompassing the defect is adaptively and automatically curved out from the entire image so that there is no need to compute singular value outside ROI. The image of defect within ROI is sub partitioned again into non-overlapping sub images. Hence, the computational complexity and time is further reduced. The exclusion of values of few dominant singular numbers depending on the number of sub images removes the grating structure and the resulting image is the image of defect. The computational complexity can be dramatically reduced from $O(M^2 \times N)$ for an entire image of size $(M \times N)$ to $O[D(m^2 \times n)]$ for D number of sub images in ROI. However, complete isolation of grating structure is not possible as such operation may fail to detect small defects in the image of test fabric. The results are obtained by running the technique over large number of samples from TILDA database which gives reasonable verification of the proposed technique.